

Grafting of Porphyrins on Cellulose Nanometric Films

Sami Boufi,[†] Manuel Rei Vilar,^{*,‡} Vicente Parra,[‡] Ana Maria Ferraria,[§] and Ana Maria Botelho do Rego[§]

Laboratoire Sciences des Matériaux et Environnement, Faculté des Sciences de Sfax, Université de Sfax, Sfax, Tunisia, ITODYS (Centre National de la Recherche Scientifique—Université Paris Diderot), Paris, France, and Centro de Química-Física Molecular, IST, Technical University of Lisbon, Lisbon, Portugal

Received March 13, 2008. Revised Manuscript Received April 24, 2008

Ultrathin films of cellulose were functionalized with iron protoporphyrin IX (FePP). Spin-coating allows the production of silylated cellulose films in a controlled way. Cellulose regeneration is achieved through the hydrolyzation of the silane groups, exposing the film to acidic vapors. To enhance the reactivity of the cellulose surface to the protoporphyrin, carbonyldiimidazole (CDI) was used as an activator. The effect of different spacers on the porphyrin grafting such as 1,8-diaminooctane and 1,4-phenylenediamine was studied. The highest level of cellulose functionalization with FePP was achieved when both the cellulose film and FePP were activated by CDI and a diaminoalkane was used as a spacer between the surface and the FePP. ATR/MIR (attenuated total reflection in multiple internal reflections) was performed in situ to follow the kinetics of the different chemical reactions with the cellulose surface. ATR/MIR proved again to be a powerful tool for probing the surface reaction. X-ray photoelectron spectroscopy permitted the elemental analysis of the cellulose surface after the chemical modification.

Introduction

Surface chemistry is currently recognized as playing a fundamental role in the changing of the chemical nature and the physical properties of materials.¹ In this domain, hybrid systems formed by inorganic substrates functionalized with organic molecules are experiencing a vast development, with main applications for chemical and biochemical sensing.² For this purpose, gallium arsenide is considered a good candidate as an inorganic semiconductor substrate given its fast electronic response.³ On the other hand, metalloporphyrins, due to their ability to coordinate gas molecules such as CO₂, NO, etc., are also widely used as organic-sensing entities.^{4–6} Studies were recently performed on these hybrid systems.^{7,8} However, some difficulties appear due to gallium arsenide's highly unstable surfaces. To overcome this problem, one has to render them reactive, ensuring their stability after the setup of the organic sensing layer. The method presented here can be generalized to other inorganic surfaces.

The difficulty of chemically modifying inorganic surfaces can be surmounted through the use of ultrathin organic films. Besides their ability to protect the surface, the presence of an organic ultrathin layer opens the way to diversify the possibility of surface modification. Among the different options, cellulose is a quite interesting medium presenting the following advantages: regular

structure; high density of hydroxyl groups on which different reactions can be carried out; high resistance to most organic solvents allowing a permanent stability of the film; excellent adhesion to inorganic substrates thanks to hydrogen bonding.

Cellulose bears three alcoholic groups per anhydroglucosic monomer: a primary and two secondary alcohol functions with different reactivity. Our former studies showed that typical reactions of cellulose, normally occurring under homogeneous conditions, can also take place on the surface.⁹ For instance, it was shown that isocyanates could react with the surface hydroxyl groups, enabling the chemical modification of the deposited film. Using diisocyanates, one can then build more complex molecular structures on the film, since one of the extremities of the chemisorbed molecule remains free for further reactions.

CDI was first used in 1960 by Paul and Anderson¹⁰ as a peptide coupling by activation of aliphatic carboxylic acids to form imidazole carboxylic esters and enabling subsequent reaction with amines. This method of activation opens the way to prepare a wide range of organic esters, carbamates, and/or amides.¹¹ This approach was successfully adopted to prepare a wide variety of cellulose ester derivatives in homogeneous solutions.¹² It is shown here that this approach permitted the chemical grafting of a porphyrin, the ferriprotoporphyrin IX chloride (hemin), on an ultrathin film of cellulose deposited on a GaAs substrate. It is also noteworthy that such a procedure permits the surface modification of cellulose ultrathin films to be held under mild conditions and room temperature, thus avoiding any risk of film alteration. These chemical reactions are illustrated in Scheme 1.

Kinetics of the different reactions performed here was studied by using in situ infrared spectroscopy in mode of attenuated total reflection in multiple internal reflections (ATR/MIR). This methodology has the advantage of following the chemisorption evolution through the absorbance measurement of a characteristic peak. Such a technique is a remarkable tool for monitoring

* Corresponding author. E-mail: manuel.rei-vilar@univ-paris-diderot.fr.

[†] Université de Sfax.

[‡] Université Paris Diderot.

[§] University of Lisbon.

(1) <http://nobelprize.org/nobel-prizes/chemistry/laureates/2007/index.html>.

(2) Cahen, D.; Hodes, G. *Adv. Mater.* **2002**, *14*, 789.

(3) Kayali, S. GaAs Material Properties. In <http://parts.jpl.nasa.gov/mm/c/>.

(4) Wu, D. G.; Cahen, D.; Graf, P.; Naaman, R.; Nitzan, A.; Shvarts, D. *Chem.—Eur. J.* **2001**, *7*, 1743.

(5) Suslick, K. S.; Rakow, N. A.; Kosal, M. E.; Chou, J.-H. *J. Porphyrins Phthalocyanines* **2000**, *4*, 407.

(6) Brunink, J. A. J.; Di Natale, C.; Bungaro, F.; Davide, F. A. M.; D'Amico, A.; Paolesse, R.; Boschi, T.; Faccio, M.; Ferri, G. *Anal. Chim. Acta* **1996**, *325*, 53.

(7) Rei Vilar, M.; El Beghdadi, J.; Debontridder, F.; Artzi, R.; Naaman, R.; Ferraria, A. M.; Botelho do Rego, A. M. *Surf. Interface Anal.* **2005**, *37*, 673.

(8) Botelho do Rego, A. M.; Ferraria, A. M.; El Beghdadi, J.; Debontridder, F.; Brogueira, P.; Naaman, R.; Rei Vilar, M. *Langmuir* **2005**, *21*, 8765.

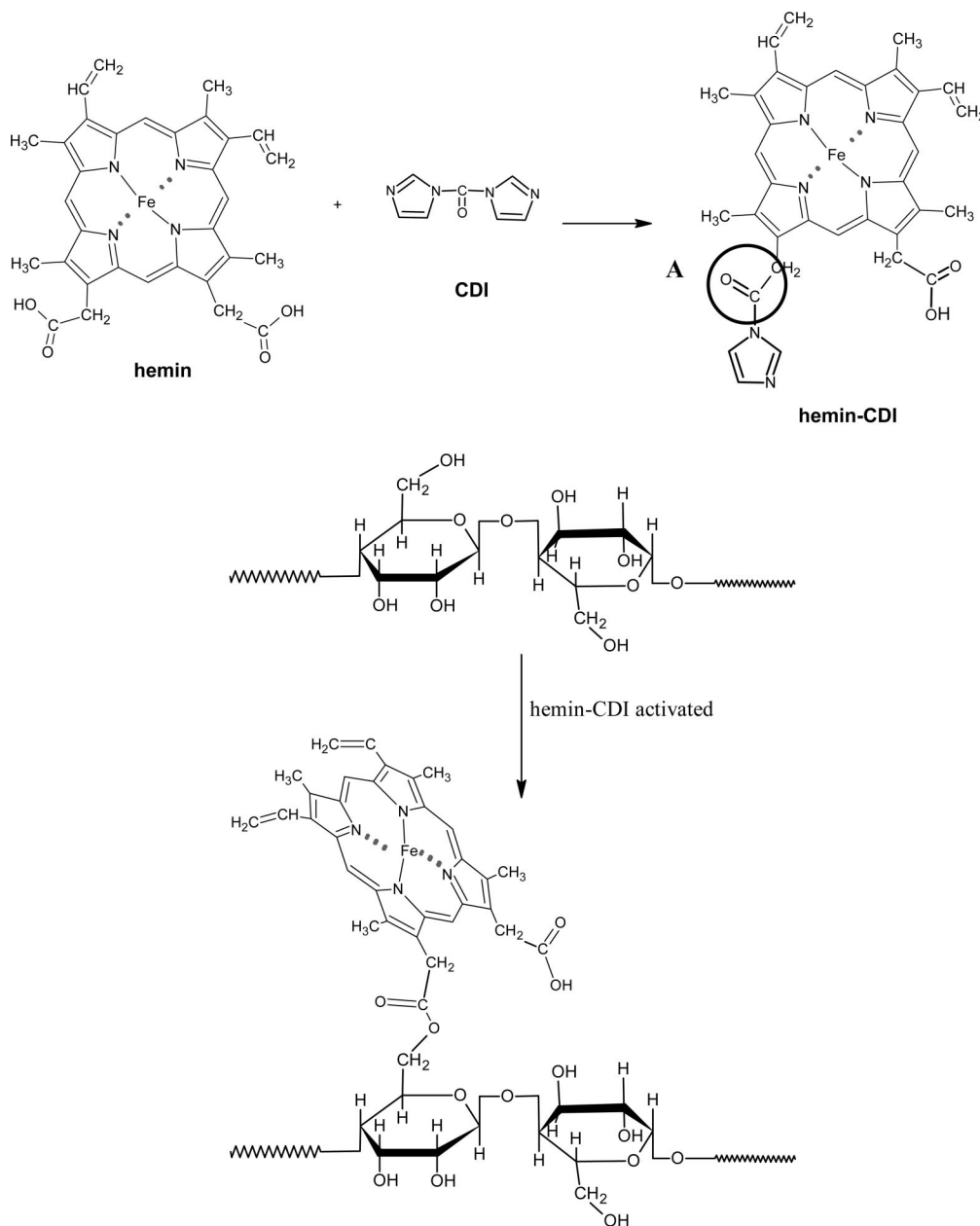
(9) Rei Vilar, M.; Boufi, S.; Ferraria, A. M.; Botelho do Rego, A. M. *J. Phys. Chem. C* **2007**, *111*, 12792.

(10) Paul, R.; Anderson, W. *J. Am. Chem. Soc.* **1960**, *42*, 4596.

(11) Rannard, S. P.; Davis, N. J. *Org. Lett.* **2000**, *2*, 2117.

(12) Liebert, T. F.; Heinze, T. *Biomacromolecules* **2005**, *6*, 333–340.

Scheme 1. CDI Activation of the FePP and Subsequent Reaction with Cellulose



reactions at a nanometric scale on semiconductor surfaces. ATR/MIR was successfully used in previous studies where isocyanate reaction with cellulose nanofilms was studied.⁹

The ensuing film was then characterized by X-ray photoelectron spectroscopy (XPS) to complement the infrared analysis by quantifying the different atomic species present on the surface.

Experimental Section

Materials and Chemicals. Undoped semi-insulating single crystal GaAs wafers with orientation (100) were acquired from Geo Semiconductors Ltd. Hemin or ferriprotoporphyrin IX chloride (FePP) was purchased from Sigma Aldrich and used as received. Anhydrous *N,N*-dimethylacetamide (DMAc) and anhydrous lithium chloride with puriss. grade were obtained from Fluka. Anhydrous dimethyl sulfoxide (DMSO), 99.7% pure, was received from Acros Organic and tetrahydrofuran (THF), analytical reagent, from Riedel de Haën. *N,N'*-Carbonyldiimidazole (CDI), 1,8-diaminooctane (DAO), and 1,4-phenylenediamine (PDA) were purchased from Aldrich. Hydrochloric acid (40%) was also purchased from Aldrich and hydrochloric acid (37%) from J.T. Baker. Deionized water with

a resistivity of 18.2 MΩ·cm was supplied through a Millipore system (Simplicity) fed with distilled water. A solution of trimethylsilyl-cellulose (TMSC) in THF (0.1 g/L) was used. The detailed procedure of the solution preparation is described elsewhere.⁹

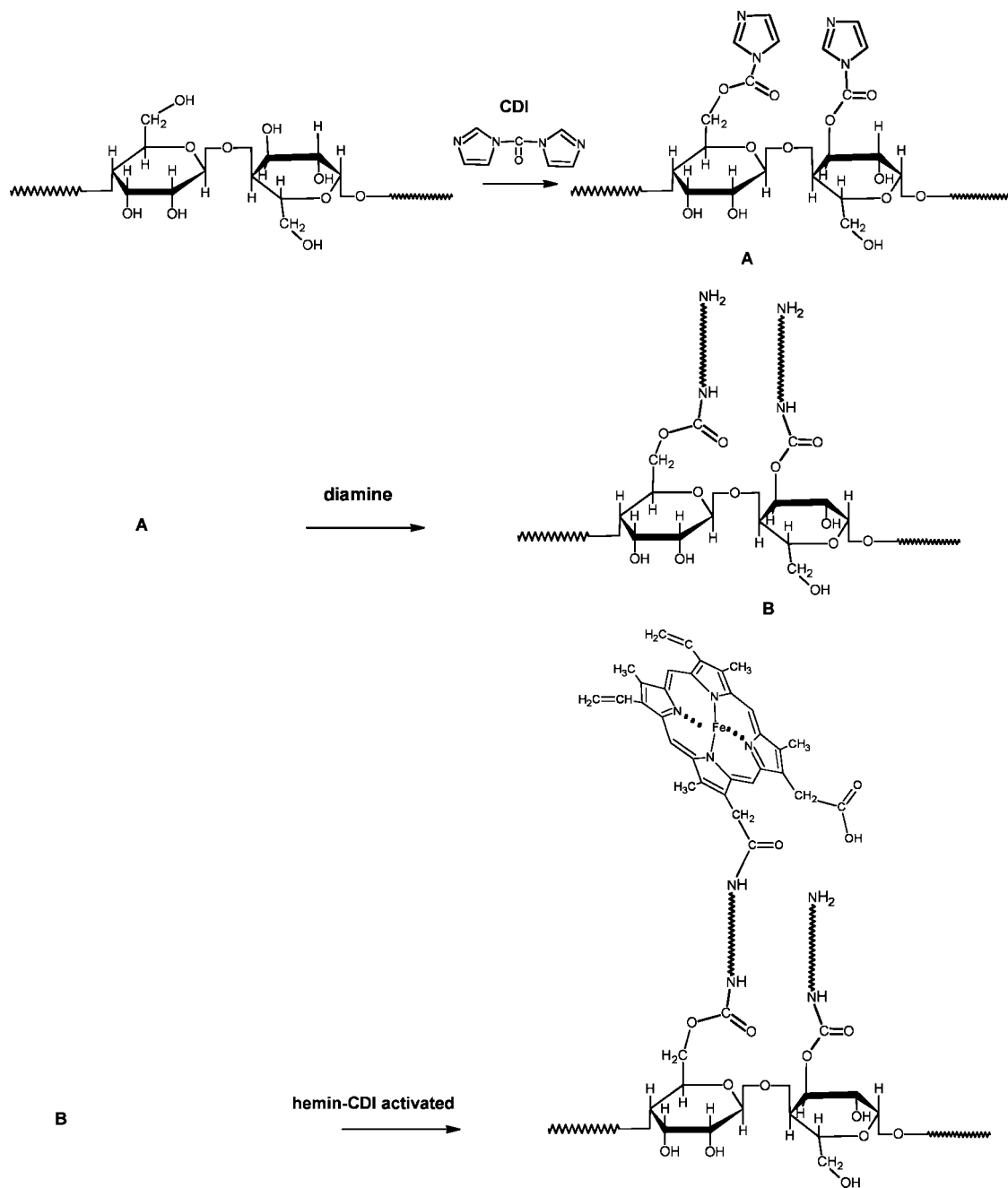
GaAs substrates were degreased using acetone and ethanol (anhydric and analytical grade from SDS) without further purification and subsequently etched in a 1% solution of hydrofluoric acid during 5 s, following a procedure described elsewhere.⁷

All thin films of TMSC were deposited by spin-coating (speed = 2000 rpm, *t* = 60 s, acceleration = 800 rpm/s) onto the etched GaAs substrates and regenerated afterward by exposing them to a saturated HCl atmosphere. ATR/MIR experiments on regenerated cellulose films (CellIR) were performed in situ. This method is described elsewhere.¹³

For XPS measurements, the following samples were prepared: (1) GaAs/CellIR in the above cited conditions; (2) GaAs/CellIR/CDI/DAO, 1,8-diaminooctane on CDI activated CellIR, cellulose film

(13) See for instance: (a) Parra, V.; Rei Vilar, M.; Battaglini, N.; Ferrara, A. M.; Botelho do Rego, A. M.; Boufi, S.; Rodríguez-Méndez, M. L.; Fonavs, E.; Muzikante, I.; Bouvet, M. *Langmuir* **2007**, 23, 3712, and references herein.

Scheme 2. CDI Activation of Cellulose and Subsequent Reaction with the 1,8- Diaminooctane, Reaction of CDI Activated Hemin with the Cellulose Surface Modified by the Alkanediamine



activated with CDI, according to Scheme 1, immersing for 2 h at 50 °C the GaAs wafer spin-coated with CellR in a solution of CDI in anhydrous DMSO (The GaAs/CellR/CDI sample was rinsed for several minutes in the solvent. Finally, the sample was introduced in a solution of DAO for 2 h at room temperature and rinsed again in anhydrous DMSO and then in dry THF.); (3) GaAs/CellR/CDI/DAO/FePP+CDI, sample prepared as described in (2) followed by interaction during 4 h at room temperature with a solution of FePP, previously CDI-activated, according to Scheme 2 (The activation of FePP was performed with a solution of CDI in anhydrous DMSO, 1:1 (v/v), during 3 h at 50 °C); (4) GaAs/CellR/CDI/PDA/FePP+CDI, the same as (3) but using 1,4-phenylenediamine instead of DAO; (5) GaAs/CellR/FePP+CDI, solution of FePP previously activated with CDI, described above, on CellR.

All chemical modification regarding treatment with CDI, amino, and hemin grafting were carried out using solutions 5×10^{-2} M.

Apparatus. An APT spin coating apparatus, a single substrate spin processor, was used for the deposition of the TMSC films.

ATR/MIR elements prepared from GaAs (100) wafers described elsewhere⁷ were covered by CellR films and used as samples. ATR/MIR spectra were recorded using a FTIRS spectrometer Magna-IR Nicolet 860 equipped with a MCT detector. Spectral resolution was 4 cm^{-1} . Kinetics of the interaction was obtained in situ. For this purpose, ATR/MIR spectra were recorded during the interaction using a homemade Teflon liquid cell provided with a hole for the introduction and extraction of the solution using a syringe. A background spectrum was recorded immediately after introducing the solution. Then, spectra were automatically recorded using a macro menu previously customized, enabling spectra acquisition at preset conditions and time. Following this procedure, one can ensure that absorbance positive (negative) peaks appearing in spectra are due to species appearing (vanishing) either on the surface region or in the neighboring interphase cellulose/solution. When consecutive interactions were performed with different solutions, intermediary rinses of the sample were carried out with the pure solvent.

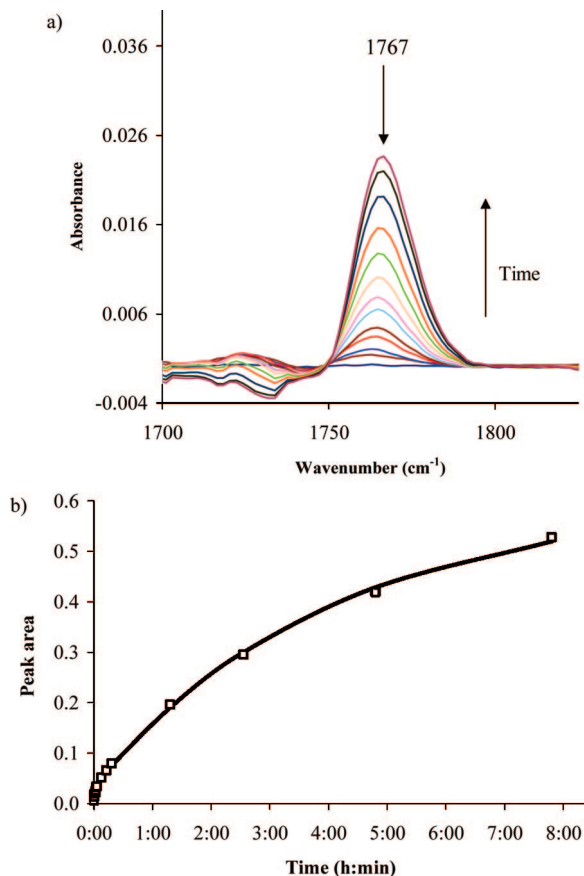


Figure 1. (a) ATR/MIR spectra in the region of C=O stretching of a cellulose film in interaction with a CDI solution in DMSO (5×10^{-2} M) showing the peak located at 1767 cm^{-1} assigned to the C=O stretching mode of the imidazole carboxylic ester generated on the cellulose surface characteristic of the cellulose activation by CDI. (b) Kinetics of the cellulose activation by CDI showing the evolution over time of the area of the peak centered at 1767 cm^{-1} (squares), fitted with eq 2.

The XPS spectrometer used was an XSAM800 (KRATOS) operated in the fixed analyzer transmission (FAT) mode, with pass energy of 20 eV. The non-monochromatized Mg K α and Al K α X-radiation ($h\nu = 1253.7$ and 1486.7 eV , respectively) were produced using a current of 10 mA and a voltage of 12 kV. Samples were analyzed using 90° and 30° takeoff angles (TOA) relative to the surface. Samples were analyzed in an ultrahigh vacuum (UHV) chamber ($\sim 10^{-7}$ Pa) at room temperature. Data acquisition and analysis details are described elsewhere.⁹ X-ray source satellites were subtracted. For quantification purposes, sensitivity factors were 0.66 for O 1s, 0.25 for C 1s, 6.3 for As $2p_{3/2}$, 4.74 for Ga $2p_{3/2}$, 0.53 for As 3d, 0.31 for Ga 3d, 0.42 for N 1s, and 3.0 for Fe $2p_{3/2}$.

Results and Discussion

FTIRS Characterization and In Situ Kinetics. It is well-known that the reaction of a carboxylic acid with an alcohol is not a spontaneous reaction. Performing these reactions in mild conditions and at room temperature is not trivial. The way to circumvent this problem, chosen in this study, consists in activating the carboxylic groups with a reagent that increases the electrophilic character of the carbonyl group. As already stated, the use of CDI as an activator appears to be an attractive approach to chemisorb a protoporphyrin on a cellulose surface. The kinetics of the CDI activation of the cellulose surface could be followed by ATR/MIR in situ. Parts a and b of Figure 1 show the spectral region containing the peak centered around 1767 cm^{-1} assigned to the C=O stretching mode of the imidazole ester generated on

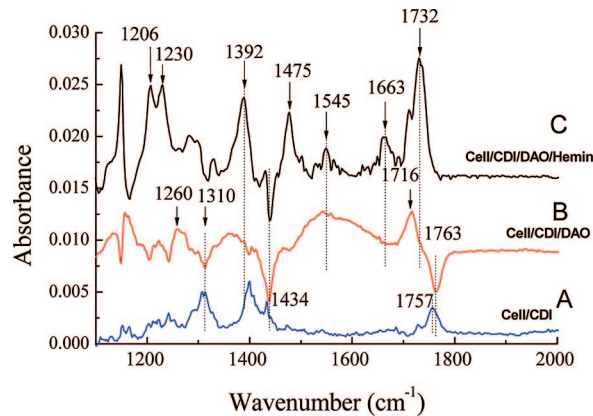


Figure 2. ATR/MIR spectra of (A) cellulose film after CDI activation, (B) CDI activated cellulose film after interaction with 1,8-diaminooctane, and (C) CDI-activated cellulose treated with 1,8-diaminooctane after interaction with hemin in DMSO.

the cellulose surface characteristic of the cellulose activation by CDI and the evolution of the area of this peak over time, respectively.

The asymmetry of the ester peak (Figure 1a) reveals the contribution of more than one component that can be assigned to the same species but under different stereochemical constraints changing over time and generating a band, which is the sum of several contributions.

The fitting of the kinetics data of the CDI activation of the surface is based on the generic function⁹

$$\Delta A = \Delta A_{\infty}(1 - \exp(-kct)) = \Delta A_{\infty}(1 - \exp(-t/\tau)) \quad (1)$$

where ΔA is the absorbance, k the kinetic constant, c the concentration of the reactive compound in solution, assumed constant during the interaction, and τ the characteristic time. However, it is worth noting here that, in cellulose, primary and secondary alcohol sites present different reactivities, as previously shown.⁹ Taking into account the existence of two chemically different sites, the following equation can be written

$$\Delta A(t) = \Delta A_{\infty}((1 - \exp(-t/\tau_1)) + f(1 - \exp(-t/\tau_2))) \quad (2)$$

used to fit experimental data (see Figure 1b), where f is the ratio between the number of reactive sites of a different nature. The activation of cellulose by CDI was found to have a “short time” term with a characteristic time, τ_1 of 2 min and a “long time” term of τ_2 equal to 4 h 04 min; f is equal to 17. The relative high value of f means that a distribution of sites of different reactivity exists. If this difference was just due to the chemical nature of primary and secondary alcohol groups, f should be 2. However, the reaction also depends on the accessibility of these sites in the cellulose surface region. Thus, the slower component corresponds to the sites less reactive, primary or secondary alcohols groups, more deeply situated in the film.

Molecular hindrance is a difficulty to be overcome when using large molecules as porphyrins. One way to avoid such porphyrin hindrance is the use of molecular spacers. 1,8-Diaminooctane and 1,4-phenylenediamine were chosen as possible spacers. For this purpose, the film was previously activated using CDI before the amine reaction according to Scheme 2.

Figure 2 shows three ATR/MIR spectra: Spectrum A corresponds to the result of the CDI activation of a cellulose film, as reported above. Characteristic peaks at 1757 , 1434 , and 1310 cm^{-1} correspond to the acyl-imidazole ester, more specifically to the C=O, imidazole cycle and C–O, respectively. Spectrum B is the result of the reaction of the 1,8-diaminooctane with a

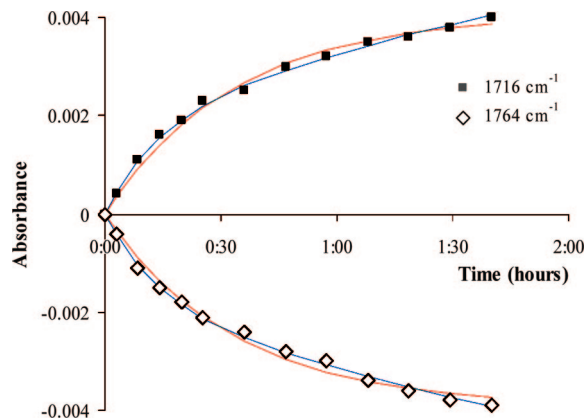


Figure 3. Kinetics of modification of the cellulose surface CDI activated with 1,8-diaminooctane in DMSO followed by ATR/MIR. The positive curve corresponds to the evolution over time of the absorbance of the peak at 1716 cm^{-1} (black squares) and the negative curve to that of the peak at 1764 cm^{-1} (white squares) characteristic of the CDI active sites in the cellulose surface. Red and blue curves fit the experimental data assuming single or double type reactive sites, respectively.

cellulose film surface previously CDI-activated. The corresponding background was recorded immediately after the CDI activation. The negative peaks at 1763 , 1434 , and 1311 cm^{-1} match well with the consumption of the CDI modified sites in the cellulose film. At 1716 and 1545 cm^{-1} one can observe typical peaks of the carbamate groups associated with C=O stretching and NH deformation, respectively. Spectrum C was recorded after the interaction of the hemin with a cellulose film previously activated with CDI and treated with 1,8-diaminooctane. The background was recorded just before the interaction with the porphyrin solution. These spectra are well-correlated to the chemisorption of the protoporphyrin according to the reaction appearing in Scheme 2B. Actually, in spectrum C, bands at 1475 and 1392 cm^{-1} and the doublet at 1230 and 1206 cm^{-1} are distinctive of the hemin.¹⁴ Otherwise, at 1663 and 1545 cm^{-1} the well-known bands of amide I and amide II appear, proofing the grafting on the 1,8-diaminooctane spacer through the creation of an amide bonding. Here again, the appearance of the band at 1732 cm^{-1} with a shoulder at 1710 cm^{-1} suggests that the protoporphyrin is physically adsorbed, as it will be mentioned below.

No reaction occurs when aromatic amines are used instead of aliphatic ones. This is mostly due to the low nucleophilic character of aromatic conjugated amines (relative to the alkylamines), which is not sufficiently high for the occurrence of the condensation reaction with the acyl-imidazole ester.

To get a better insight into the procedure, kinetics of the reaction of the aliphatic amine with the surface were followed by ATR/MIR in situ. Figure 3 displays the kinetics of the appearance of the carbamate carbonyl corresponding to the peak at 1716 cm^{-1} and the simultaneous disappearing feature at 1764 cm^{-1} relative to the acyl-imidazole ester. The symmetry of the two curves is quite striking suggesting that the disappearance of the carbonyl in the acyl-imidazole ester is highly correlated with the appearance of the carbonyl in the carbamate group. This also implies that carbamate group appears as a result of the acyl-imidazole ester consumption.

Two different assumptions were used for the data fitting, regarding the reactivity of the CDI modified sites in the cellulose surface relatively to the amine: (1) All the acyl-imidazole ester sites have the same reactivity. In this case, eq 1 is used. (2) Acyl-imidazole ester sites, created in primary and secondary

alcohols of cellulose, display two different reactivities. Here, eq 2 has to be applied.

With assumption 1, positive and negative absorbance values were fitted either separately or simultaneously. Separate fitting of ascending and descending curves has different characteristic times of $\tau_1 = 31 \pm 2$ and $\tau_2 = 35 \pm 2$ min. In the second case, ascending and descending curves were constrained to have the same characteristic time, resulting in $\tau = 33 \pm 2$ min (red curve in Figure 3). This value is comparable to τ_1 and τ_2 , found in the separate fitting, confirming that the disappearance and the appearance of species happen in the same step. With assumption 2, the number of parameters to fit is larger. Hence, only the simultaneous fitting was performed giving characteristic times of $\tau_1 = 14$ min and $\tau_2 = 4\text{ h } 47\text{ min}$, and $f = 4$. Both assumptions lead to fittings presenting high correlation factors: $r = 0.9989$ using assumption 2 and $r = 0.9964$ using assumption 1. The lower value of f when compared to that obtained with the CDI activation translates the fact that in this reaction—amine with CDI activated cellulose surfaces—kinetics depends more strongly on the chemical nature of the sites than on their accessibility. This is due to the high nucleophilic character of the amino group and to the fact that acyl-imidazole esters are now more exposed than hydroxyl groups in the cellulose surface.

A spectrum after the interaction of the hemin with the cellulose film, where 1,8-diaminooctane molecules were previously grafted, was already presented in Figure 2. As described above, characteristic bands located at 1732 , 1663 , and 1545 cm^{-1} attest to the grafting of the porphyrin on the cellulose film. Moreover, the doublet centered around 1210 cm^{-1} is a breathing deformation mode of the porphyrin ring and the peak at 1392 cm^{-1} is a symmetric deformation of CH_3 adjacent groups of the porphyrin molecule. The shoulder around 1710 cm^{-1} corresponds to carbamate groups formed by the reaction between one of the hemin carboxylic groups and imidazole. As stated above, peaks at 1710 and 1732 cm^{-1} are typical of C=O stretching modes of the unreacted carbonyl groups of the hemin, belonging, respectively, to carboxyl groups that were CDI activated (group A encircled in Scheme 1) or to those that remained free. Since the concentrations of CDI and hemin used in the activating solution are the same, we would expect that one carboxylic group per hemin molecule reacts, in average, with CDI. Hence, being physically adsorbed, each molecule contributes to the absorbance increase corresponding to both modes. However, the activated carboxylic group can react with free amine group and instead of the typical vibrations at 1710 , other modes at 1663 and 1545 cm^{-1} appear, which correspond to the amide formation through the C=O stretching and the NH bending, respectively.

In Figure 4, the evolution of the four above-mentioned modes is shown. The increase of both peaks at 1663 and 1545 cm^{-1} attests to the occurrence of a condensation reaction between the unreacted amine extremity of the previously grafted diamino alkyl chain and the hemin activated carboxylic group. The presence of the peaks at 1732 and 1710 cm^{-1} is associated with the physical adsorption of the hemin before reaction with the amine group on the cellulose surface. The rapid increase of absorbance of both peaks in the first minutes of interaction shows that the physisorption of the hemin molecules is much faster than their chemical reaction. However, after this rapid initial rise, instead of a plateau, it exhibits a slight increase that is here attributed either to a swelling of the cellulose film with consequent penetration of the hemin or to a reorientation of the hemin molecules, which allow further sites to be occupied. If the activation was efficient, the intensity of the peak at 1710 cm^{-1} should follow the same evolution as that of the peak at 1732

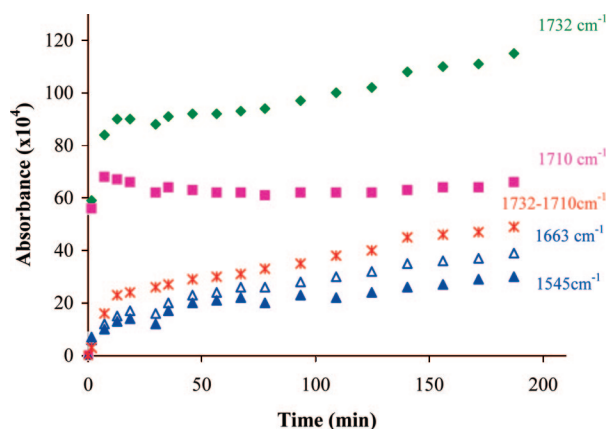


Figure 4. Kinetics of the hemin adsorption on a cellulose surface modified by 1,8-diaminooctane based on the evolution of absorbance of characteristic bands corresponding to the amide formation, located at 1548 and 1665 cm^{-1} , and those of unreacted (CDI activated) and free carboxyl groups at 1710 cm^{-1} and 1732 cm^{-1} , respectively. Data “1732–1710 cm^{-1} ” correspond to the difference between absorbance of bands located at 1732 and 1710 cm^{-1} .

cm^{-1} subtracted from the reacted amount. The difference between them should give the rate of disappearance of the activated group, assuming that the absorption coefficient of both carbonyl groups are the same in both the activated and free groups and that hemin molecules contain, on average, one activated and one free carboxylic group. This rate should be the same as the rate of appearance of the carbonyl in the amide group (peak at 1663 cm^{-1}). In fact, as shown in Figure 4, the evolution of this difference is comparable to that of the peak at 1663 cm^{-1} , attesting to a very efficient activation and confirming the assumptions above. The fact that the physical adsorption is much faster than the chemical reaction proves that the chemical reaction of the porphyrins with the amine is not controlled by diffusion.

XPS Characterization. Table 1 displays the main quantitative results from XPS: nitrogen and iron amounts reported to carbon, the most abundant element both in the cellulose film and in the reactive molecules. The ratio N/Fe, the estimated thicknesses, and the covered fraction f are also included.

Thicknesses were estimated considering an island-like adsorption neglecting shadow effects.¹⁵ Calculated atomic ratios were fitted to experimental atomic ratios C/Ga, N/Ga, C/As, and N/As considering nonoxidized peaks of Ga 3d and As 3d. The fitting was performed using a nonlinear least-squares method with the following parameters: the covered fraction f , thickness, and ratio between the atomic densities $n_X/n_{\text{Ga(orAs)}}$.

The estimated thickness of the regenerated cellulose films (CellR) varies between 6 and 7 nm for a single spin-coated deposition of silylated cellulose. The absence of silicon (not

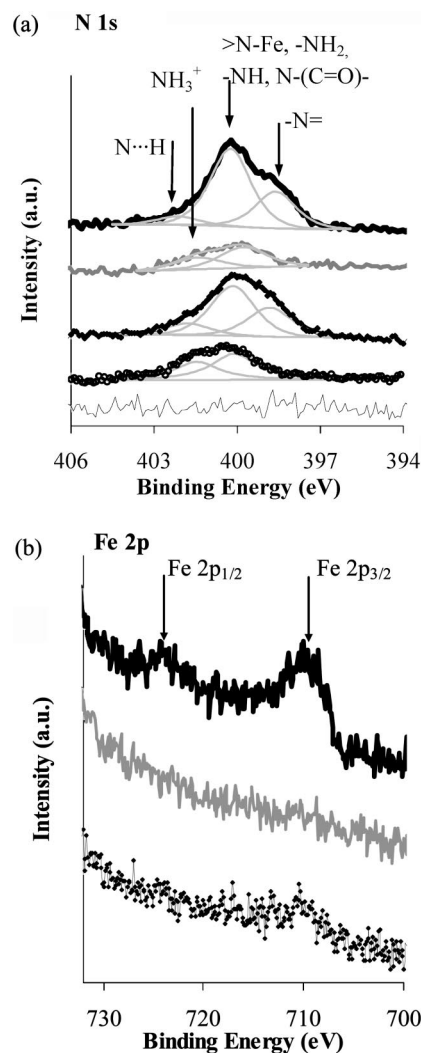


Figure 5. XPS (a) N 1s and (b) Fe 2p regions. From top to bottom: CellR/CDI/DAO/FePP + CDI, CellR/CDI/PDA/FePP + CDI, and CellR/FePP + CDI. In the N 1s region two further spectra are shown: CellR/CDI/DAO and, at the bottom, CellR.

shown) in the spectrum shows that the cellulose was fully regenerated. The covered fraction is higher than 0.9. The estimated thickness does not change, within the experimental error, after activation (with CDI) and functionalization (with DAO). Anyway, the maximum length of the DAO + carbamate group is around 1 nm, and the N 1s XPS region (Figure 5a) confirms beyond any doubt the presence of the diamine on the cellulose. The efficiency of the adsorption of a porphyrin such as iron protoporphyrin (hemin), which has two carboxylic groups, depends on several

Table 1. Estimated Thicknesses, Covered Fractions, and Experimental Atomic Ratios^a

		CellR	CellR/CDI/DAO	CellR/CDI/DAO/FePP + CDI	CellR/CDI/PDA/FePP + CDI	CellR/FePP + CDI
thickness ± 1 nm		6	7	9	5	8
covered fraction, $f \pm 0.02$		0.94	0.93	0.97	0.88	0.98
atomic ratio	TOA, deg	CellR	CellR/CDI/DAO	CellR/CDI/DAO/FePP + CDI	CellR/CDI/PDA/FePP + CDI	CellR/FePP + CDI
N/C	90	<i>b</i>	0.10	0.13	0.07	0.11
	30		0.07	0.12	0.07	0.06
Fe/C ($\times 10^3$)	90	<i>c</i>	<i>c</i>	3.7	<i>c</i>	1.8
	30			4.3		1.5
N/Fe	90			36		59
	30			27		42

^a The experimental data were obtained with the X-ray Mg source. The TOAs are 90° and 30°. (The atomic concentrations obtained at 90° are representative of a larger depth than at 30°). ^b No nitrogen detected; ^c No iron detected.

factors. The study presented here focused on the role of the type of diamine spacer used on the chemisorption of previously CDI activated hemin.

On comparison of the N 1s region of the sample grafted with DAO with the one with DAO and FePP + CDI (second and fifth spectra from bottom in Figure 5a, respectively), the sample without hemin clearly contains two components: one (present in both samples) centered around 400 eV that includes the contributions of amine groups, imidazole rings, and urethane groups (from 399 to 400.3 eV one can find all these contributions) and another one centered at 401.6 eV typical of N⁺. This component can be the result of NH₂ group ionization, explaining why it appears in the sample without hemin where the amine groups are free and exposed, while in the sample with hemin these groups are used to graft the porphyrin forming carbamate groups (–NH–CO–). The N 1s region of CellR/CDI/DAO/FePP + CDI sample was fitted with three different peaks: the peak centered at 398.6 eV assigned to aromatic nitrogen, the peak around 400 eV including the contribution of N bound to Fe, carbamate groups (NH(CO)O), and likely N of unreacted CDI imidazole groups as well as unreacted –NH₂ groups, and a third component centered at 402.2 eV usually assigned to shakeup satellites.¹⁶ However, in the range 401.5–405 eV, several authors have also pointed out nitrogen involved in hydrogen bonds.¹⁷ But the real fingerprint of hemin is iron. The detection of Fe 2p (Figure 5b, first spectrum from the top) confirms the presence of the hemin on the film. This is in agreement with the ATR/MIR results confirming that the porphyrin is undoubtedly grafted. The highest coverage level of FePP is observed when an aliphatic diamino spacer is previously grafted on the cellulose film. This can be imputed to the amino group's higher reactivity toward acyl-imidazole ester relative to the hydroxyl groups of the cellulose surface and also to the lower steric interaction among porphyrin molecules when they are grafted on the amines. Also, the chemisorption of FePP possessing a high molecular dimension is less problematic when flexible aliphatic chains, which are relatively long (formed by eight methylene groups), are present on the surface. This makes the encounter between the amino terminal groups and the FePP more likely.

Finally, the hemin grafting strongly depends on the type of spacer used. When the sample prepared with DAO is compared with the one prepared with an aromatic diamine, like 1,4-phenylenediamine (PDA), it is clear from the Fe 2p region that the sample prepared with PDA does not have the porphyrin bound

to the surface (Figure 5b, second from the top). Conversely, the presence of iron is very clear in the sample prepared with the aliphatic diamine. As was mentioned before, the presence of the aromatic group lowers the reactivity of the amine groups due to the conjugated system. In order to quantify the iron, a single component was fitted in Fe 2p_{3/2}, but it also contains other features mainly due to multiplet splitting effects. The absence of hemin in the sample prepared with aromatic diamine is also confirmed by the XPS regions C 1s (not shown) and N 1s (similar to that obtained with CellR/CDI/DAO without hemin) and concords with the thickness estimation, 5 ± 1 nm against ~9 nm with DAO. The porphyrin alone has a length of 1.57 nm. Adding the length of DAO + carbamate groups, the maximum length DAO/FePP + CDI would be around 3 nm. When aromatic diamine is used, the Auger peak assigned to the Ga LMM of the substrate is detected in the tail of the C 1s region. However, when 1,8-diaminooctane is used, this structure of Ga is not visible, indicating that the substrate is better covered. It seems that the interaction between the cellulose film and the solutions has removed some material from the sample, since both the estimated thickness and covered fraction have slightly decreased relative to the CellR sample. Nevertheless, the difference between the thicknesses of these samples is within the estimation error.

Conclusions

Grafting of iron protoporphyrin IX (FePP) on nanofilms of cellulose was achieved through the activation of the cellulose surface with CDI. Two different pathways have been considered: (i) FePP activated by CDI followed by reaction with the cellulose film; (ii) activation of the cellulose film with CDI followed by the reaction with diamines and then the reaction with FePP activated by CDI. Infrared analysis and XPS data confirmed the occurrence of FePP grafting through all the procedures, the second one being the most efficient when an aliphatic diamine is used as the spacer. Recourse to diamines as spacers resulted in a real improvement in the rapidity and efficiency of porphyrin grafting on cellulose surfaces. Actually, porphyrin chemisorption on the cellulose film is practically accomplished after half an hour of interaction.

Acknowledgment. We thank NATO project (CBP.MD. CLG982316), the bilateral cooperation of Ministère de la Recherche Scientifique, Technologique et de Développement des Compétences (Tunisia) with GRICES (Portugal), Grant TP/20065, the project DGRST/CNRS (France), Grant 06R 12-06, and the FCT postdoctoral grant (A.M.F.), SFRH/BPD/26239/2006, for financial support.

LA800786S

(15) Rei Vilar, M.; Botelho do Rego, A. M.; Ferraria, A. M.; Jugnet, Y.; Noguès, C.; Peled, D.; Naaman, R. *J. Phys. Chem. B* **2008**, *112*, 6957.

(16) Berríos, C.; Cárdenas-Jirón, G. I.; Marco, J. F.; Gutiérrez, C.; Ureta-Zañartu, M. S. *J. Phys. Chem. A* **2007**, *111*, 2706, and references therein.

(17) Botelho do Rego, A. M.; Pereira, L. P.; Reis, M. J.; Oliveira, A. S.; Vieira Ferreira, L. F. *Langmuir* **1997**, *13*, 6787, and references therein.